JOURNAL OF GEOPHYSICAL RESEARCH, VOL. 102, NO. D22, PAGES 25,915–25,926, NOVEMBER 27, 1997

# Correction of Rayleigh scattering effects in cloud optical thickness retrievals

Menghua Wang

University of Maryland Baltimore County, NASA Goddard Space Flight Center, Greenbelt, Maryland

Michael D. King

Earth Sciences Directorate, NASA Goddard Space Flight Center, Greenbelt, Maryland

**Abstract.** We present results that demonstrate the effects of Rayleigh scattering on the retrieval of cloud optical thickness at a visible wavelength (0.66 $\mu$m). The sensor-measured radiance at a visible wavelength (0.66 $\mu$m) is usually used to infer remotely the cloud optical thickness from aircraft or satellite instruments. For example, we find that without removing Rayleigh scattering effects, errors in the retrieved cloud optical thickness for a thin water cloud layer ($\tau_c = 2.0$) range from 15 to 60%, depending on solar zenith angle and viewing geometry. For an optically thick cloud ($\tau_c \gtrsim 10$), on the other hand, errors can range from 10 to 60% for large solar zenith angles ($\theta_0 \gtrsim 60°$) because of enhanced Rayleigh scattering. It is therefore particularly important to correct for Rayleigh scattering contributions to the reflected signal from a cloud layer both (1) for the case of thin clouds and (2) for large solar zenith angles and all clouds. On the basis of the single scattering approximation, we propose an iterative method for effectively removing Rayleigh scattering contributions from the measured radiance signal in cloud optical thickness retrievals. The proposed correction algorithm works very well and can easily be incorporated into any cloud retrieval algorithm. The Rayleigh correction method is applicable to cloud at any pressure, providing that the cloud top pressure is known to within $\pm$100 hPa. With the Rayleigh correction the errors in retrieved cloud optical thickness are usually reduced to within 3%. In cases of both thin cloud layers and thick clouds with large solar zenith angles, the errors are usually reduced by a factor of about 2 to over 10. The Rayleigh correction algorithm has been tested with simulations for realistic cloud optical and microphysical properties with different solar and viewing geometries. We apply the Rayleigh correction algorithm to the cloud optical thickness retrievals from experimental data obtained during the Atlantic Stratocumulus Transition Experiment (ASTEX) conducted near the Azores in June 1992 and compare these results to corresponding retrievals obtained using 0.88 $\mu$m. These results provide an example of the Rayleigh scattering effects on thin clouds and further test the Rayleigh correction scheme. Using a nonabsorbing near-infrared wavelength (0.88 $\mu$m) in retrieving cloud optical thickness is only applicable over oceans, however, since most land surfaces are highly reflective at 0.88 $\mu$m. Hence successful global retrievals of cloud optical thickness should remove Rayleigh scattering effects when using reflectance measurements at 0.66 $\mu$m.

## 1. Introduction

In the remote sensing of cloud microphysical, optical, and radiative properties from aircraft or satellite sensors, the sensor-measured radiance at visible wavelengths (0.66 $\mu$m) is primarily a function of cloud optical thickness, whereas near-infrared (NIR) radiances (1.6, 2.1, and 3.7 $\mu$m) are sensitive both to optical thickness and, especially, to cloud particle size [*Foot*, 1988; *Nakajima and King*, 1990; *Nakajima and Nakajima*, 1995; *Platnick and Valero*, 1994; *Twomey and Cocks*, 1982, 1989]. As a consequence, Rayleigh scattering in the atmosphere above the cloud primarily affects the cloud optical thickness retrieval since the Rayleigh optical thickness in the near-infrared is negligible. Because the Rayleigh optical thickness in the visible wavelength region is small (about 0.044 at 0.66 $\mu$m), it has previously been neglected in retrieving cloud optical thickness. In principle, one can also retrieve the cloud optical thickness using a nonabsorbing NIR band (e.g., 0.88 $\mu$m) over the ocean. Rayleigh scattering has much less effect on cloud optical thickness retrievals at 0.88 $\mu$m than at 0.66 $\mu$m since the Rayleigh optical thickness is much smaller ($\tau_r \sim 0.015$ at 0.88 $\mu$m). Over land, however, it is preferable to use visible wavelengths (0.66 $\mu$m) because the surface reflectance of land is low at this wavelengths, in contrast to NIR bands where the surface reflectance can reach 0.5 over vegetation areas. In this paper we investigate the Rayleigh scattering effects on cloud optical thickness retrievals at a visible (0.66 $\mu$m) wavelength for various cloud microphysical and optical properties and different solar and viewing geometries. We then propose a scheme to effectively remove the Rayleigh scattering contributions. Finally, we extensively test the Rayleigh correction algorithm with simulations and provide results of retrieving cloud optical thickness from experimental measurements



Paper number 97JD02225.
0148-0227/97/97JD-02225$09.00

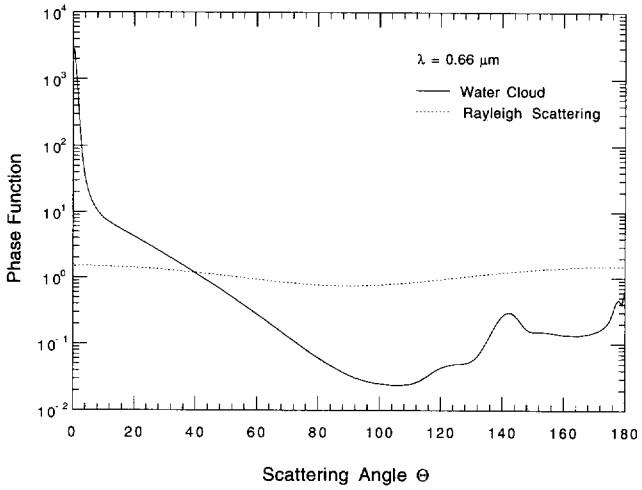


**Figure 1.** Phase function as a function of scattering angle for air molecules (Rayleigh scattering) and a water cloud at $\lambda$ = 0.66 $\mu$m. The water cloud is assumed to have an effective particle radius of 8.0 $\mu$m.

obtained during Atlantic Stratocumulus Transition Experiment (ASTEX) in June 1992.

## 2. Cloud-Ocean-Atmosphere System

We begin with the definition of the reflectance $R = \pi I/F_0 \cos\theta_0$, where $I$ is the radiance in the given viewing direction, $F_0$ is the extraterrestrial solar irradiance, and $\theta_0$ is the solar zenith angle. With this normalization for $I$, $R$ determined at the top of the atmosphere (TOA) would be the albedo of the atmosphere if $I$ were independent of viewing angle. In the remote sensing of cloud optical and radiative properties from aircraft or satellites the measured reflectance at the visible wavelength (e.g., 0.66 $\mu$m) is primarily used to retrieve cloud optical thickness, whereas NIR reflectances (1.6, 2.1, and 3.7 $\mu$m) are primarily used to retrieve cloud particle size. Therefore molecular scattering above the cloud primarily affects the cloud optical thickness retrieval. Figure 1 illustrates the phase functions of air molecules (Rayleigh scattering) as well as for a typical water cloud at 0.66 $\mu$m with an effective particle radius $r_e$ = 8.0 $\mu$m. Note that in the range of scattering angles that are generally accessible for satellite remote sensing (~100°–160°), values of the Rayleigh scattering phase function are about 1–2 orders of magnitude larger than those of the water cloud, which predominantly scatters in the forward direction. Since the upward reflectance at visible wavelengths at the TOA is proportional to the product of phase function and slant path optical thickness ($\tau_r/\cos\theta_0$), Rayleigh scattering contributions are important for cases of both thin clouds and large solar zenith angles for all clouds.

To understand the cloud-ocean-atmosphere system and to carry out the radiative transfer simulations described below, a model of the vertical structure of the cloud-atmosphere system above the surface is needed. Usually, stratocumulus water clouds are confined to a layer around 1–2 km, with more than 80% of the Rayleigh scattering occurring above the cloud. Thus it is reasonable to simplify the cloud-atmosphere system as a two-layer model with air molecules above the cloud. The scattering processes contributing to the upward reflectance at the TOA can be approximated by a two-layer cloud-atmosphere system composed of air molecules, a water cloud, and cloud-atmosphere interactions. We can write the total upward reflectance (ignoring Sun glitter) at visible wavelengths at the top of the cloud-ocean-atmosphere system, for viewing and solar zenith angles $\theta$ and $\theta_0$ and relative azimuth angle $\Delta\phi$, as

$$R_t(\tau_r, \tau_c; \theta, \theta_0, \Delta\phi) = R_r(\tau_r; \theta, \theta_0, \Delta\phi) + R_{rc}(\tau_r, \tau_c; \theta, \theta_0, \Delta\phi) + T(\tau_r; \theta)R_c(\tau_c; \theta, \theta_0, \Delta\phi)T(\tau_r; \theta_0), \quad (1)$$

where $R_r$ is the reflectance resulting from multiple scattering by air molecules (Rayleigh scattering) in the absence of the cloud, $R_c$ is the reflectance resulting from multiple scattering by the cloud in the absence of the air, $R_{rc}$ is multiple interaction term between air molecules and clouds, $\tau_r$ and $\tau_c$ are the Rayleigh and cloud optical thicknesses, respectively, and $T(\tau_r; \theta_0) = \exp(-\tau_r/\cos\theta_0)$ is the direct transmittances of the air molecules. It is understood that $R_t$, $R_{rc}$, and $R_c$ in (1) also depend weakly on cloud effective particle radius $r_e$ at the visible and nonabsorbing NIR wavelengths. The Rayleigh scattering reflectance $R_r$ varies nearly as the inverse fourth power of wavelength and contributes equally to the forward and backward scattering directions. The optical properties of Rayleigh scattering are well known and can be computed accurately [*Hansen and Travis*, 1974]. The term $R_{rc}$ accounts for the interactions between Rayleigh scattering and clouds, e.g., photons first scattered by air molecules and then scattered by clouds or photons scattered by clouds and then air molecules. $R_c$ denotes the upward reflectance at the top of the cloud (TOC) and is primarily a function of the cloud optical thickness. This term is used to derive $\tau_c$ from reflected solar radiation measurements. For thin clouds, $R_c$ is proportional to the cloud optical thickness $\tau_c$, and hence errors in $R_c$ lead proportionally to errors in the retrieved optical thickness $\tau_c$. For thicker clouds ($\tau_c \gtrsim 8$), on the other hand, the cloud reflectance at the TOC can be written as asymptotic expression where the $\tau_c$ dependent term is proportional to $-\tau_c^{-1}$ [*King*, 1987]. Therefore $\Delta R_c \propto \tau_c^{-2}\Delta\tau_c$, and the error in retrieved optical thickness is $\propto \tau_c^2\Delta R_c$.

Consider an atmosphere composed of air molecules and water clouds bounded by the ocean, where $R_t$ represents the satellite measured reflectance. We denote $R_t^{(\mathrm{meas})}$ and $R_c^{(\mathrm{meas})}$ as upward reflectances measured by the sensor at the TOA and the TOC, respectively. We can estimate the error involved in retrieving the cloud optical thickness without Rayleigh correction, i.e., converting cloud optical thickness directly from $R_t^{(\mathrm{meas})}$ instead of $R_c^{(\mathrm{meas})}$. Define $\Delta R = R_t^{(\mathrm{meas})} - R_c^{(\mathrm{meas})}$. We can write $\Delta R$ from (1) as

$$\Delta R(\tau_r, \tau_c; \theta, \theta_0, \Delta\phi) = R_r(\tau_r; \theta, \theta_0, \Delta\phi) + R_{rc}(\tau_r, \tau_c; \theta, \theta_0, \Delta\phi) + R_c^{(\mathrm{meas})}(\tau_c; \theta, \theta_0, \Delta\phi) \cdot [T(\tau_r; \theta)T(\tau_r; \theta_0) - 1]. \quad (2)$$

It is interesting to note that Rayleigh scattering effects do not always enhance the total TOA reflectance $R_t$. Obviously, contributions from the first two terms ($R_r + R_{rc}$) and the last term in $\Delta R$ in (2) are in opposite directions. The last term in (2) is always negative, becoming increasing negative as $\theta$ and/or $\theta_0$ increase. On the other hand, for a given value of $\theta$ and $\theta_0$, the larger the cloud reflectance $R_c^{(\mathrm{meas})}$ at the TOC, the larger is the negative value of this term. Together, with both large $\theta$

(and/or $\theta_0$) and $R_c^{(meas)}$, $\Delta R$ could become negative (i.e., $R_t^{(meas)} < R_c^{(meas)}$). Both enhancement and reduction of reflectance are possible because the Rayleigh phase function is symmetric and very bland, whereas the cloud phase function is very strongly forward biased. Consequently, Rayleigh scattering can add reflectance where the cloud is reflecting weakly but acts to remove stronger directional cloud scatter from the view direction.

## 3. Radiative Transfer Code

We developed a matrix operator (adding-doubling) code to solve the scalar radiative transfer equation (RTE) for a plane-parallel atmosphere bounded by a smooth Fresnel-reflecting ocean. This code computes the upwelling radiance at the top and downwelling at the base of the medium with any number of layers in the atmosphere. Several tests have been carried out to validate the accuracy of the computational method and the code. First, the results were compared with the successive orders of scattering code [*Gordon and Wang*, 1992; *Wang*, 1991] of a two-layer atmosphere bounded by a flat ocean for various atmospheric profiles and different solar and viewing geometries. The results agreed with one another to within 0.1%. Next, with larger aerosol optical thicknesses ($\tau_a = 2.0$), the results were compared with computations from the forward Monte Carlo (FMC) code from K. Ding and H. R. Gordon (personal communication, 1996) at the University of Miami for various solar and viewing geometries. Again, the results agreed with one another to within ~0.1%. Finally, with a water cloud layer of $\tau_c = 4$ and 10 and no reflecting boundary surface at the bottom, the results were checked with calculations from the discrete ordinates method (DOM) from *Nakajima and Tanaka* [1986] for solar zenith angles $\theta_0 = 0°$ and 60° and various viewing geometries. Most of these results agreed with one another to ~0.3%. The maximum difference in upward reflectance was 0.59%. We conclude from these tests that the adding-doubling code is capable of yielding radiances that are accurate to at least ~0.3%.

## 4. Error in Retrieved $\tau_c$ Without Rayleigh Correction

We have used our adding-doubling code to compute reflectances $R_t^{(meas)}$ of a two-layer cloud-ocean-atmosphere model and $R_c^{(meas)}$ of a one-layer cloud bounded by a flat Fresnel-reflecting ocean for various cloud optical thicknesses $\tau_c$ and different solar and viewing geometries at $\lambda = 0.66$ μm. These computations used a Rayleigh optical thickness of $\tau_r = 0.044$ for the top layer. With $R_c^{(meas)}$ as the reference library for different values of $\tau_c$, $R_t^{(meas)}$ can be converted to cloud optical thickness $\tau_c^{(meas)}$ by neglecting Rayleigh scattering effects above the cloud. Errors in the retrieved cloud optical thickness without Rayleigh correction $\Delta\tau_c = \tau_c^{(meas)} - \tau_c$ were then obtained. Figures 2a and 2b are contour plots showing typical errors (in percent) in retrieved $\tau_c$ without making any Rayleigh corrections. These examples apply to the case of cloud with an effective particle radius $r_e = 8.0$ μm. Figure 2a is for cases of $\Delta\tau_c$ (in percent) for different solar and viewing zenith angles when $\tau_c = 2.0$, while Figure 2b is $\Delta\tau_c$ (in percent) for different solar angles and various cloud optical thicknesses when viewing zenith angle $\theta = 45.2°$. Figure 2a shows that for a thin cloud, $\Delta\tau_c$ ranges from 15 to 60% for solar and viewing zenith angle ranges from 0 to 80°. Errors increase with increasing solar and/or viewing angles because of enhanced Rayleigh scattering contributions at large angles. On the other hand, Figure 2b shows that for thick clouds, $\Delta\tau_c$ still can be as high as 10–60% for solar zenith angles $\theta_0 \gtrsim 60°$. It is therefore important to correct for Rayleigh scattering contributions in the case of thin clouds for all solar zenith angles and for large solar zenith angles and all clouds.

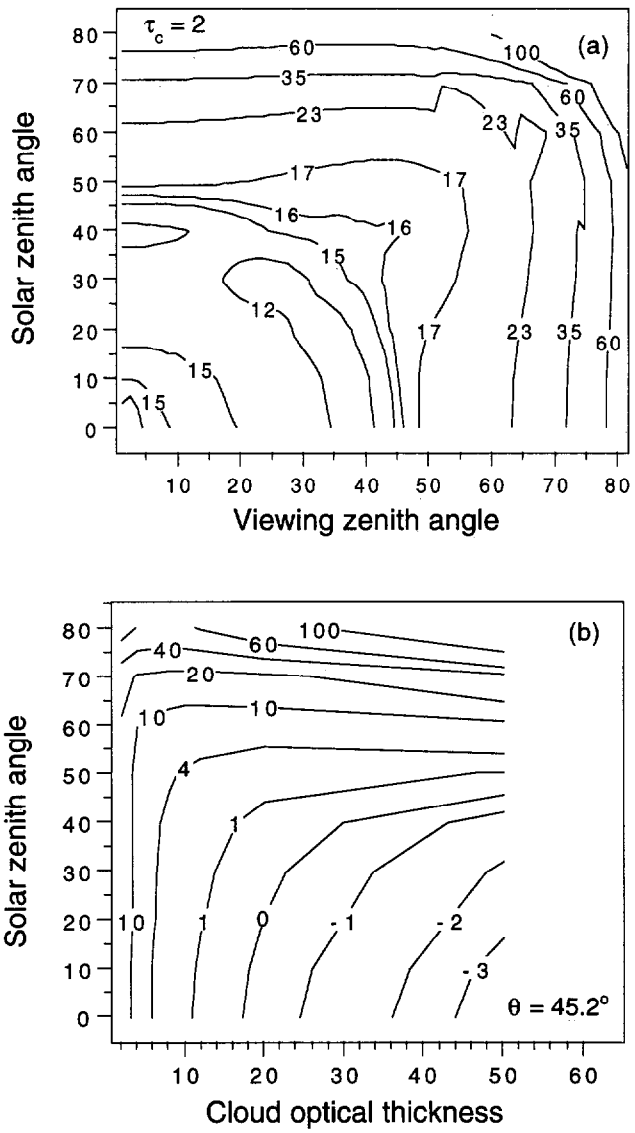


**Figure 2.** Error $\Delta\tau_c$ (in percent) in retrieved cloud optical thickness without making any Rayleigh corrections for (a) $\tau_c = 2.0$ and (b) $\theta = 45.2°$. $\Delta\phi = 90°$ in both cases.

Though much reduced, the errors in retrieved cloud optical thickness using a nonabsorbing NIR (0.88 μm) wavelength over oceans are still significant. We found from simulations that the errors $\Delta\tau_c$ in retrieved cloud optical thickness at $\lambda = 0.88$ μm are about 5% for thin clouds ($\tau_c = 2$) for $\theta_0 \leq 60°$. The error reduced to about 2% for $\tau_c = 4$. For clouds with large solar zenith angles ($\theta_0 \geq 60°$), however, $\Delta\tau_c$ ranges from 5 to 25% (see the appendix). Therefore, for nonabsorbing NIR bands (0.88 μm) it is still important to correct for Rayleigh scattering effects in deriving cloud optical thickness, especially for large solar zenith angles ($\theta_0 \gtrsim 60°$).

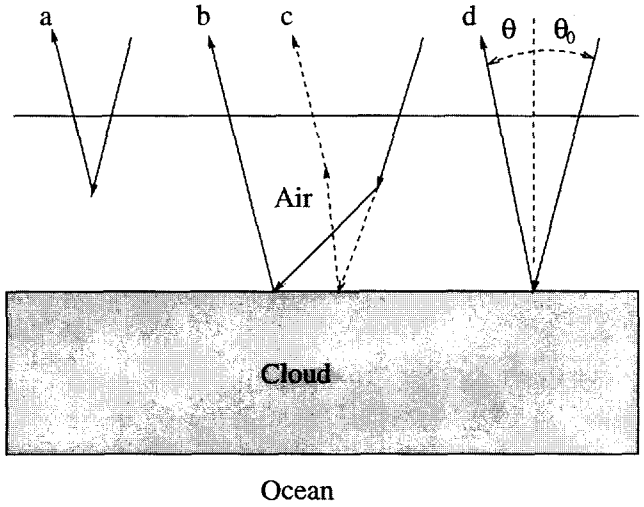


**Figure 3.** Single scattering processes of upward reflectance in the cloud-ocean-atmosphere system.

## 5. Rayleigh Correction Scheme

In this section we first derive an expression for $R_t$ in the cloud-ocean-atmosphere system with the Rayleigh single scattering approximation; next, we discuss approximations for multiple scattering contributions and propose an iterative method for making Rayleigh scattering corrections in cloud optical thickness retrievals; and finally, we give some test results from the simulations.

### 5.1. Single Scattering Approximation

Since the Rayleigh optical thickness at 0.66 $\mu$m is small, we begin with the single scattering approximation in which photons are only scattered once in the air molecule layer above the cloud. Because of its simplicity, we use single scattering theory as guidance for deriving cloud top reflectance from measured total reflectance at the TOA. The single scattering approximation is valid if both slant path $\tau_r/\cos\theta$ and $\tau_r/\cos\theta_0$ are small.

In the Rayleigh single scattering and cloud-atmosphere single interaction approximations, the upward reflectances of the two-layer cloud-ocean-atmosphere system are composed of four parts as shown in Figure 3: term a, direct Rayleigh single scattering without reflection from the cloud; term b, single scattering in the air toward the cloud followed by reflection from the cloud; term c, reflection of the direct solar beam from the cloud followed by single scattering in the air; and term d, reflection of the direct solar beam from the cloud. We can write these four terms as

$$R^{(a)}(\tau_r;\ \theta,\ \theta_0,\ \Delta\phi) = \frac{\tau_r P_-(\theta,\ \theta_0,\ \Delta\phi)}{4\cos\theta\cos\theta_0}, \tag{3}$$

$$R^{(b)}(\tau_r,\ \tau_c;\ \theta,\ \theta_0) = \frac{\tau_r}{4\pi\cos\theta_0}\,T(\tau_r;\ \theta) \cdot \int_{\Omega/2} P_-(\theta',\ \theta_0,\ \Delta\phi')\,R_c(\tau_c;\ \theta,\ \theta',\ \Delta\phi')\,d\Omega', \tag{4}$$

$$R^{(c)}(\tau_r,\ \tau_c;\ \theta,\ \theta_0) = \frac{\tau_r}{4\pi\cos\theta}\,T(\tau_r;\ \theta_0) \cdot \int_{\Omega/2} P_+(\theta,\ \theta',\ \Delta\phi')\,R_c(\tau_c;\ \theta',\ \theta_0,\ \Delta\phi')\,d\Omega', \tag{5}$$

$$R^{(d)}(\tau_r,\ \tau_c;\ \theta,\ \theta_0,\ \Delta\phi) = T(\tau_r;\ \theta)\,R_c(\tau_c;\ \theta,\ \theta_0,\ \Delta\phi)\,T(\tau_r;\ \theta_0), \tag{6}$$

where $P_{\pm}$ is the Rayleigh scattering phase function in the forward (positive) and backward (negative) scattering directions, respectively. The integrals in (4) and (5) are difficult to compute since the exact reflection function $R_c(\tau_c;\ \theta,\ \theta',\ \Delta\phi')$ is usually unknown. As an approximation to these integrals, we assume that the upward reflectance at the cloud top is independent of the viewing angle, that is, the integral can be approximated by the product of cloud albedo $A_c$ and integration of the Rayleigh phase function. We can then approximate $R^{(b)}$ and $R^{(c)}$ in (4) and (5) as

$$R^{(b)}(\tau_r,\ \tau_c;\ \theta,\ \theta_0) \approx \frac{\tau_r}{2\cos\theta_0}\,T(\tau_r;\ \theta)A_c(\tau_c;\ \theta), \tag{7}$$

$$R^{(c)}(\tau_r,\ \tau_c;\ \theta,\ \theta_0) \approx \frac{\tau_r}{2\cos\theta}\,T(\tau_r;\ \theta_0)A_c(\tau_c;\ \theta_0), \tag{8}$$

where $A_c(\tau_c;\ \theta_0)$ is the cloud albedo for optical thickness $\tau_c$ and solar incident angle $\theta_0$. In (7) and (8), $R^{(b)}$ and $R^{(c)}$ represent interactions involving photons that interact only once between air molecules and clouds. They are independent of the azimuthal angle $\Delta\phi$ since photons lose their memory of $\Delta\phi$ when interacting with clouds (air molecules) from scattering by air molecules (clouds). The total reflectance at the TOA with the Rayleigh single scattering approximation can thus be written as

$$R_t(\tau_r,\ \tau_c;\ \theta,\ \theta_0,\ \Delta\phi) = \frac{\tau_r P_-(\theta,\ \theta_0,\ \Delta\phi)}{4\cos\theta\cos\theta_0} + \frac{\tau_r}{2\cos\theta_0}A_c(\tau_c;\ \theta)\exp(-\tau_r/\cos\theta) + \frac{\tau_r}{2\cos\theta}A_c(\tau_c;\ \theta_0)\exp(-\tau_r/\cos\theta_0) + R_c(\tau_c;\ \theta,\ \theta_0,\ \Delta\phi)\exp\left[-\tau_r\left(\frac{1}{\cos\theta}+\frac{1}{\cos\theta_0}\right)\right]. \tag{9}$$

Note that $R_t$ in the above is symmetric in $\theta$ and $\theta_0$, as required by the Helmholtz principle of reciprocity.

### 5.2. Multiple Scattering

When we consider multiple scattering in the cloud-ocean-atmosphere system, we replace (9) by (1); that is, reflectances resulting from Rayleigh single scattering and single interaction of the cloud-atmosphere in (9) are replaced by multiple scattering and multiple interaction counterparts, respectively. For the multiple scattering case, there is no simple way of deriving the total reflectance $R_t$ explicitly. However, the Rayleigh multiple scattering and cloud-atmosphere multiple interaction contributions usually increase the total reflectance at the TOA. It is therefore possible to modify (9) in such a way as to approximate multiple scattering effects. In the appendix we show that the single scattering approximation given by (9) works quite well. Most importantly, we show that with the single scattering Rayleigh correction, the errors in cloud top reflectance are quite constant with various cloud optical thick-

nesses and different solar and viewing geometries. Thus we find it is reasonable to rewrite the last term in (9) as

$$R^{(d)}(\tau_r, \tau_c; \theta, \theta_0, \Delta\phi) = R_c(\tau_c; \theta, \theta_0, \Delta\phi) \cdot \exp\left[-C_m\tau_r\left(\frac{1}{\cos\theta} + \frac{1}{\cos\theta_0}\right)\right] \quad (10)$$

where $0 < C_m < 1$ is a constant accounting for multiple scattering effects. Finally, the cloud top reflectance $R_c$ can be derived from (9) by replacing the last term by (10):

$$R_c^{(\text{calc})}(\tau_c; \theta, \theta_0, \Delta\phi) = \left(R_t^{(\text{meas})}(\tau_r, \tau_c; \theta, \theta_0, \Delta\phi) - \left[\frac{\tau_r P_-(\theta, \theta_0, \Delta\phi)}{4\cos\theta\cos\theta_0} + \frac{\tau_r}{2\cos\theta_0}A_c(\tau_c; \theta)\exp(-\tau_r/\cos\theta) + \frac{\tau_r}{2\cos\theta}A_c(\tau_c; \theta_0)\exp(-\tau_r/\cos\theta_0)\right]\right) \cdot \exp\left[C_m\tau_r\left(\frac{1}{\cos\theta} + \frac{1}{\cos\theta_0}\right)\right]. \quad (11)$$

This is the equation for the Rayleigh scattering correction in the cloud optical thickness retrievals. Note that $\tau_r$ in (11) is the Rayleigh optical thickness from the cloud top to the top of the atmosphere. It can be estimated by

$$\tau_r = \frac{p_c}{p_0}\tau_{r0}, \quad (12)$$

where $p_0$ and $p_c$ are the atmospheric pressures at the surface and at the TOC, respectively, and $\tau_{r0}$ is the Rayleigh optical thickness at the atmospheric pressure $p_0$ which is usually taken as the standard atmospheric pressure of 1013 hPa. It is obvious from (11) and (12) that the Rayleigh scattering contributions above the cloud are related to cloud top pressure. The $C_m$ value in (11) can be derived empirically from simulations. The exact value of $C_m$ in (11) is usually dependent on the solar and viewing geometries as well as cloud optical and microphysical properties. However, we have found from simulations that there exists a rather constant value of $C_m$. In the appendix we show that the $C_m$ value is only weakly dependent on the cloud optical thickness and the solar and viewing geometry. We also show in the appendix that the $C_m$ value is nearly independent of the cloud top pressure $p_c$, i.e., the value of Rayleigh optical thickness $\tau_r$. Except as noted in the appendix, all results presented in this paper used $\tau_r = 0.044$ (applicable to $\lambda = 0.66$ $\mu$m and $p_c = p_0$) and $C_m = 0.84$.

### 5.3. Test of Equation (11) With Simulations

We test the accuracy of (11) by comparing the cloud top reflectance $R_c$ from (11) and from direct computations. We first compute $R_t^{(\text{meas})}$ in (11) by solving the RTE using the adding-doubling code for a two-layer cloud-ocean-atmosphere system, where clouds are in the lower layer, overlying a flat Fresnel-reflecting ocean. $R_t^{(\text{meas})}$ was simulated as the sensor measured upward radiance at the TOA. Cloud top reflectance $R_c^{(\text{calc})}$ can then be computed using (11) with $C_m = 0.84$ as discussed in section 5.2. We also computed the cloud top reflectance $R_c^{(\text{meas})}$ by solving the RTE with the adding-doubling code for a one-layer cloud over a flat Fresnel-reflecting ocean. The $R_c^{(\text{meas})}$ was simulated as sensor measured radiance at the TOC. The difference defined as $\Delta R_c = R_c^{(\text{calc})} - R_c^{(\text{meas})}$ is calculated. Using $R_c^{(\text{meas})}$ as lookup libraries, $R_c^{(\text{calc})}$ can be converted to cloud optical thickness $\tau_c^{(\text{calc})}$. The error in retrieved cloud optical thickness can therefore be computed as $\Delta\tau_c = \tau_c^{(\text{calc})} - \tau_c$, where $\tau_c$ is the true cloud optical thickness to compute $R_c^{(\text{meas})}$.

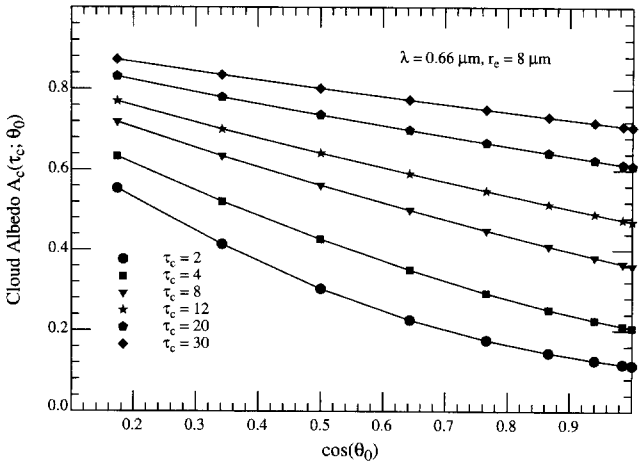


**Figure 4.** Cloud albedo $A_c$ as a function of the cosine of the solar zenith angle $\theta_0$ for various cloud optical thicknesses $\tau_c$.

To compute the $R_c^{(\text{calc})}$ through (11), we need values of cloud albedo $A_c$. In the visible band (0.66 $\mu$m) the cloud albedo $A_c$ is primarily a function of the solar zenith angle $\theta_0$ and cloud optical thickness $\tau_c$. It is weakly dependent on the cloud effective particle radius $r_e$. Figure 4 illustrates the cloud albedo $A_c$ as a function of cosine of the solar zenith angle for cloud effective particle radius $r_e = 8$ $\mu$m for various cloud optical thicknesses. The $A_c$ values in Figure 4 were computed using an adding-doubling code for a one-layer cloud over a flat Fresnel-reflecting ocean. It is interesting to note that for a given cloud optical thickness the cloud albedo can be approximately linearly related to the cosine of the solar zenith angle. In particular, for thick clouds (e.g., $\tau_c \gtrsim 6$), cloud albedos $A_c$ can be computed accurately using the asymptotic formula [*van de Hulst*, 1980; *King*, 1987]. In all results discussed in this paper, we used $A_c$ values for $r_e = 8.0$ $\mu$m shown in Figure 4 for deriving $R_c^{(\text{calc})}$ and $\tau_c^{(\text{calc})}$ for cases of various cloud optical and microphysical properties and different solar and viewing geometries.

Figure 5 gives examples of $\Delta R_c$ and $\Delta\tau_c$ for cases of both thin and thick cloud layers for different solar and viewing geometries. For comparison purposes, errors are presented for both cases with and without Rayleigh corrections. The abscissa in Figure 5 is the solar zenith angle ($\theta_0$) for azimuthal angle of $\Delta\phi = 0°$ ($\theta_0 < 0°$) and 180° ($\theta_0 \geq 0°$). The ordinate is the errors in $\Delta R_c$ or $\Delta\tau_c$. Figure 5 has a cloud effective particle radius of $r_e = 8.0$ $\mu$m and a viewing zenith angle $\theta = 45.2°$. It is obvious from Figure 5 that (11) is exceptionally good at removing Rayleigh scattering contributions for both thin and thick cloud layers. The errors $\Delta R_c$ were corrected to within 2% for both thin and thick clouds (within 1% in most cases), while the errors in $\tau_c$ were reduced to within 3% in most cases. The error in the retrieved cloud optical thickness was usually reduced by

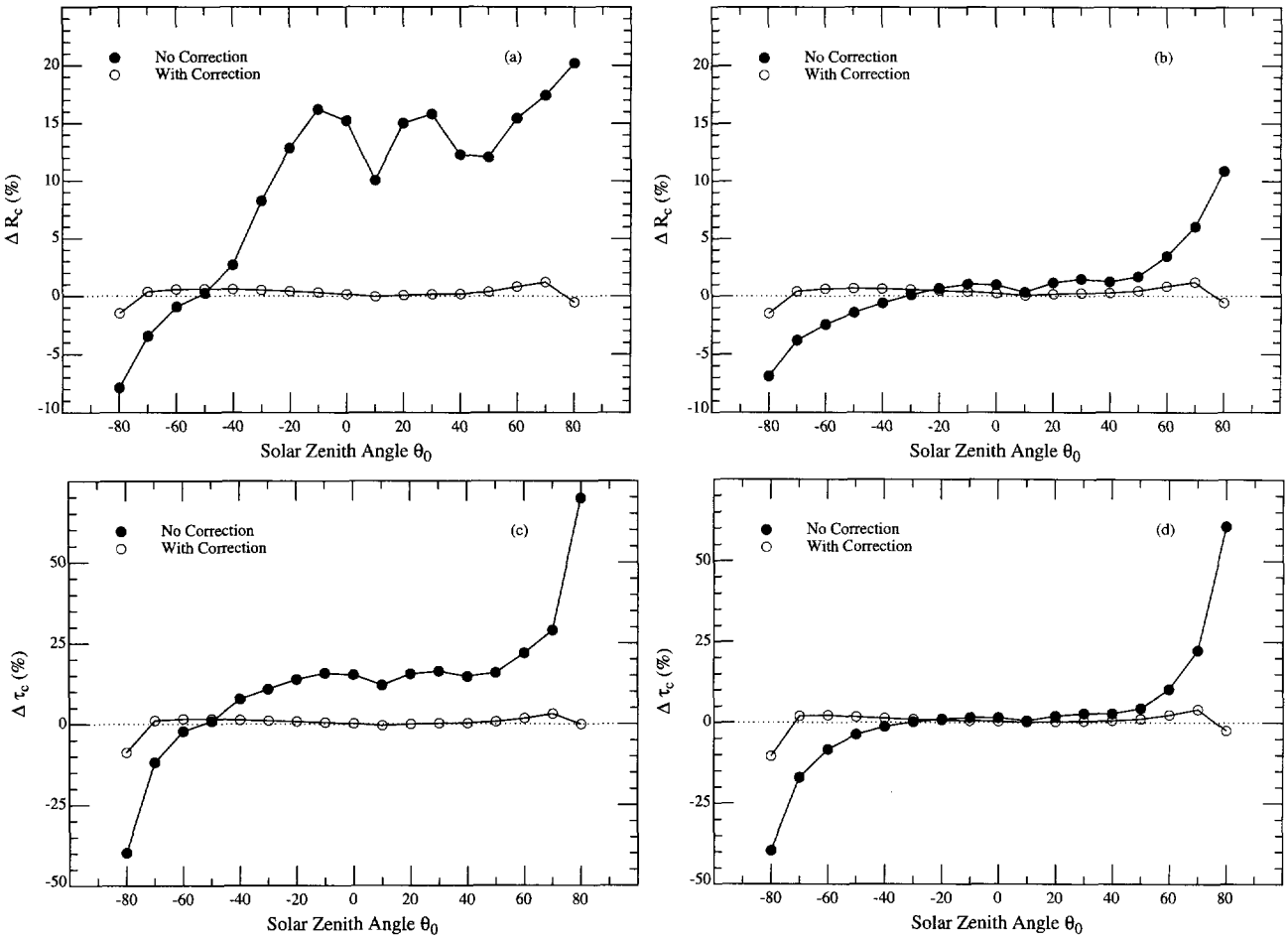


**Figure 5.** Error $\Delta R_c$ ($\Delta \tau_c$) (in percent) for $\theta = 45.2°$ and $\Delta\phi$ of 0° ($\theta_0 < 0°$) and 180° ($\theta_0 \geq 0°$) as a function of the solar zenith angle for (a) $\tau_c = 2$ ($\Delta R_c$); (b) $\tau_c = 10$ ($\Delta R_c$); (c) $\tau_c = 2$ ($\Delta \tau_c$); and (d) $\tau_c = 10$ ($\Delta \tau_c$).

a factor of about 2 to over 10 in cases of both thin cloud layers and optically thick clouds with large solar zenith angles.

### 5.4. Rayleigh Correction Algorithm

As noted in section 5.3, to correct for Rayleigh scattering contributions using (11), the cloud albedo $A_c$ for the solar and viewing zenith angles is required. The cloud albedo $A_c$ depends on the cloud optical thickness which is unknown a priori. We found it efficient to compute $R_c^{(\text{calc})}$ using (11) with iteration. The procedure can be schematically described as

$$R_t^{(\text{meas})} \rightarrow [\tau_c^{(i)} \rightarrow A_c^{(i)} \rightarrow R_c^{(i)}]$$

where the right-hand side (in brackets) is iteration with (11) and $i = 0, 1, 2 \cdots$. The case of $i = 0$ refers to no Rayleigh correction. It usually converges within two iterations ($i = 2$).

Implementation of the Rayleigh correction scheme into any cloud retrieval algorithm is straightforward. The Rayleigh correction can be incorporated into the procedure prior to the cloud retrievals. First, with precalculated cloud albedo libraries as shown in Figure 4, the sensor-measured reflectance $R_t^{(\text{meas})}$ at a visible wavelength can be used to estimate $R_c^{(\text{calc})}$ by going through the Rayleigh correction algorithm. Next, the corrected TOC reflectance $R_c^{(\text{calc})}$ can be used as input to the cloud retrievals.

## 6. Simulated Results

We have performed simulations of cloud optical thickness retrievals using the Rayleigh correction scheme outlined in section 5.4 for various cloud microphysical and optical properties and for different solar and viewing geometries. Figures 6a–6d are histograms of the number of retrievals as a function of $\Delta \tau_c$ (in percent) for various cloud optical thicknesses for solar zenith angle $\theta_0 = 70°$. For comparison purposes, we also plotted histograms of $\Delta \tau_c$ (in percent) for cloud optical thickness retrievals without making any Rayleigh correction. In generating Figure 6, we used two iterations ($i = 2$) and precalculated the cloud albedo assuming $r_e = 8$ $\mu$m as shown in Figure 4 for the computation of $R_c^{(\text{calc})}$ in (11). For a given solar zenith angle $\theta_0$, there are a total of 444 retrievals in the plot for viewing zenith angles $\theta = 1.0°$–$45.2°$ (at steps of about 1°); azimuthal angles $\Delta\phi = 0°$, 90°, and 180°; and cloud effective particle radii $r_e = 4$, 8, 16, and 32 $\mu$m. Figures 6a–6d show errors $\Delta \tau_c$ in the cloud optical thickness retrievals for $\tau_c = 2$, 6, 10, and 20, respectively.

These results demonstrate that the Rayleigh correction algorithm is quite effective in reducing bias errors associated with molecular scattering above clouds. For thin cloud layers the error $\Delta \tau_c$ is reduced in most cases from about 30% to 2–3% for $\tau_c = 2$ and 15% to 1–2% for $\tau_c = 6$, while for the

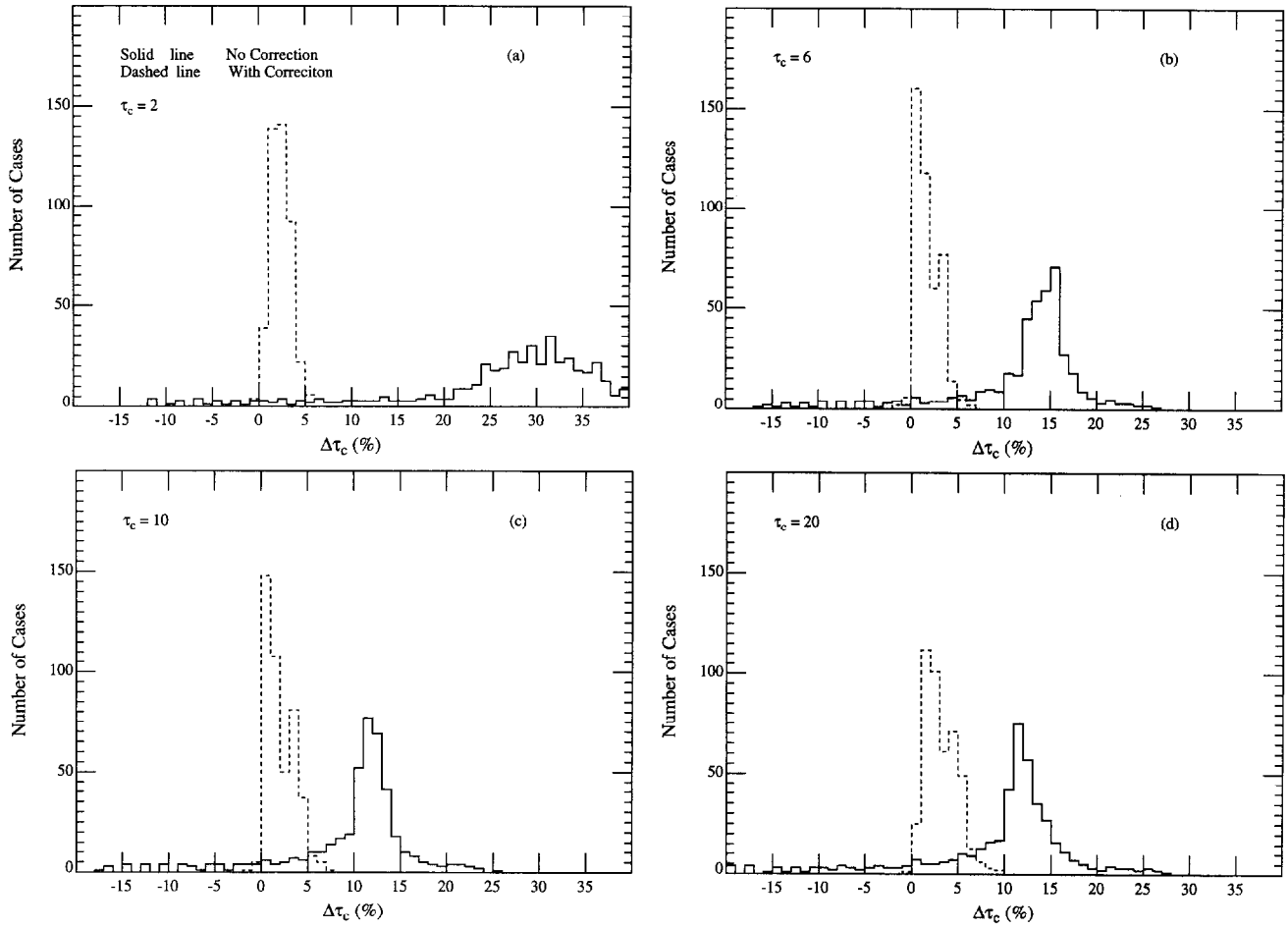


**Figure 6.** Number of cases as a function of $\Delta\tau_c$ (in percent) for $\theta_0 = 70°$ and (a) $\tau_c = 2$; (b) $\tau_c = 6$; (c) $\tau_c = 10$; and (d) $\tau_c = 20$. This includes total of 444 retrievals for cases of $\theta = 1.0°$–$45.2°$; $\Delta\phi = 0°$, 90°, and 180°; and $r_e = 4$, 8, 16, and 32 $\mu$m.

cases of thick clouds and large solar zenith angle ($\theta_0 = 70°$) the $\Delta\tau_c$ is reduced in most cases from about 12% to 1–2% for both $\tau_c = 10$ and 20. Note that (11) corrects for Rayleigh reflectance contributions. Errors in $R_c$ after Rayleigh correction are much less than those in $\tau_c$, particularly for the cases of thick clouds and large solar zenith angles. Table 1 shows the largest errors of $\Delta\tau_c$ and $\Delta R_c$ obtained both with and without Rayleigh corrections. These are the largest errors in $R_c$ and $\tau_c$ encountered for each figure and includes result from 444 simulated retrievals for various cloud effective particle radii and different viewing geometries. The largest errors in $\tau_c$ and $R_c$ in Figure 6a, for example, are 5.6% and 4.2% (with Rayleigh correction) and 40.0% and 38.4% (without Rayleigh correction), respectively. The largest errors were reduced by about factor of 7–9 in Figure 6a. On the other hand, Figure 6d indicates that for thick clouds the largest errors for both $\tau_c$ and $R_c$ were reduced by about a factor of 2–3. Note that the largest error in $R_c$ in Figure 6d was corrected to 2.2%, which is the smallest in Table 1. This is because for thick clouds (in the asymptotic range) the cloud top reflectance $R_c$ is much less sensitive to changes of the cloud optical thickness $\tau_c$. Therefore small changes of $\Delta R_c$ result in large changes of $\Delta\tau_c$. Results show that the Rayleigh correction algorithm works very well for various cloud optical and microphysical properties and different solar and viewing geometries. In particular, knowledge of cloud optical thickness and effective particle radius is not required in the Rayleigh corrections. Statistically, one usually overestimates the cloud optical thickness without the Rayleigh correction. Therefore one can expect that without this correction, remote sensing values of the cloud optical thickness at large latitudes tend to be overestimated.

**Table 1.** Largest Errors in $\tau_c$ and $R_c$ in Figures 6a–6d for Cases With and Without Rayleigh Corrections

| | With Correction | | No Correction | |
|---|---|---|---|---|
| Figure | $\Delta\tau_c$ | $\Delta R_c$ | $\Delta\tau_c$ | $\Delta R_c$ |
| 6a | 5.6 | 4.2 | 40.0 | 38.4 |
| 6b | 6.2 | 2.6 | 26.7 | 11.7 |
| 6c | 7.2 | 2.3 | 25.1 | 7.8 |
| 6d | 9.5 | 2.2 | 27.4 | 5.6 |

In percent.

## 7. Observation and Validation With ASTEX Data

To further test the correction algorithm and validate the Rayleigh scattering effects on the retrieval of cloud radiative

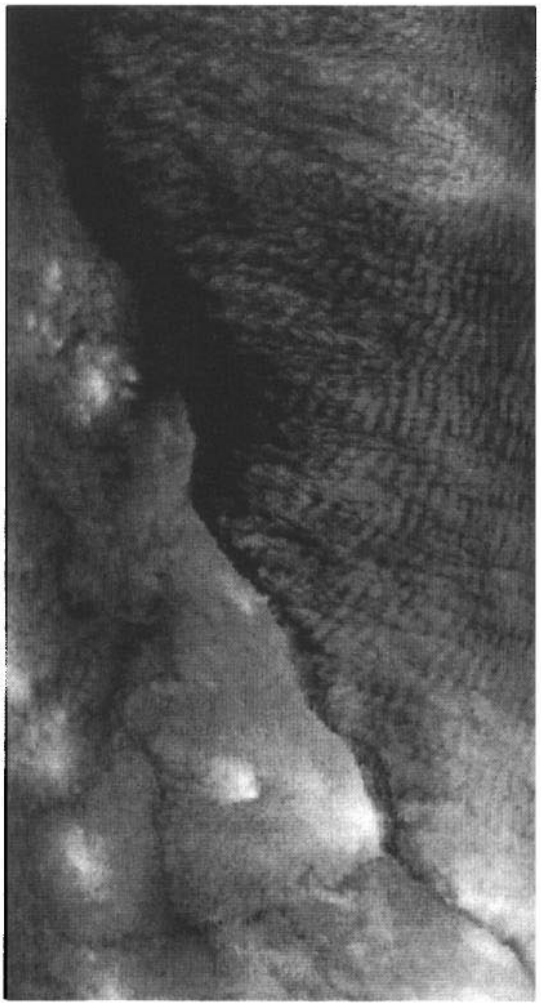

**Figure 7.** Visible (0.66 $\mu$m) image acquired during ASTEX on June 17, 1992, between 1221:21 and 1226:21 UTC. The solar zenith angle for this flight line was about 20°. This image is about 37 km cross track and 62 km along track (down length of image).

properties, we implemented the Rayleigh correction into the cloud retrieval algorithm of *Nakajima and King* [1990] using the measured radiances at a visible and an absorbing NIR (2.1 $\mu$m) band. Briefly, the cloud retrieval algorithm operates first by converting the measured radiance at a visible wavelength to cloud optical thickness. Then the cloud effective particle radius can be retrieved from both measured radiance at the NIR (2.1 $\mu$m) wavelength and cloud optical thickness from the visible through comparison with precalculated lookup radiance library. For thin clouds the measured radiance at the absorbing NIR band depends both on the cloud optical thickness and effective particle radius, whereas for thick clouds it depends only on the cloud effective particle radius. Therefore, for thin clouds the errors in cloud optical thickness lead to errors in the retrieved cloud effective particle radius. We applied the cloud retrieval algorithm with our Rayleigh correction scheme to the problem of retrieving cloud optical thickness and effective particle radius from experimental data obtained during the Atlantic Stratocumulus Transition Experiment (ASTEX) conducted near the Azores in June 1992. We used measurements obtained from the moderate-resolution imaging spectrometer (MODIS) airborne simulator (MAS) [*King et al.*, 1996] that was flown on the NASA ER-2 aircraft at an altitude of around 20 km. The MAS has a 2.5-mrad instantaneous field of view and scans perpendicular to the aircraft flight track with a scan angle of ±43° about nadir, thereby providing images with a spatial resolution of 50 m at nadir.

During ASTEX, the MAS measured upward radiances in 11 spectral channels from the visible through the thermal infrared. In particular, it recorded the visible radiances centered at 0.66 and 0.88 $\mu$m with bandwidths of 0.05 and 0.04 $\mu$m, respectively. Figure 7 shows a MAS visible (0.66 $\mu$m) image acquired on June 17, 1992, between 1221:21 and 1226:21 UTC. The solar zenith angle in this flight was about 20°. To observe the Rayleigh scattering effects, we performed cloud optical thickness and effective particle radius retrievals for all pixels for which $2 \leq \tau_c \leq 5$ and $4 \leq r_e \leq 26$. The cloud effective particle radius was obtained using the MAS measured radiance at 2.1 $\mu$m and optical thickness obtained from the visible or a nonabsorbing NIR wavelength. We retrieved cloud optical thickness using the MAS visible measurements at 0.66 $\mu$m for cases both with and without Rayleigh corrections and for near-infrared measurements at 0.88 $\mu$m without Rayleigh corrections. Figures 8a and 8b show the probability distribution func-

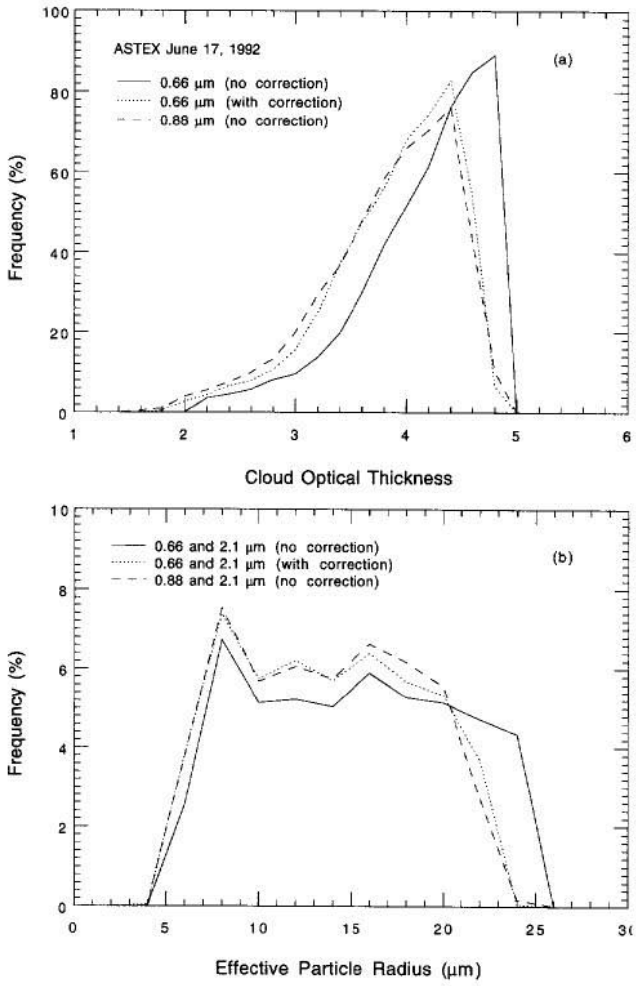


**Figure 8.** Probability distribution function of (a) retrieved cloud optical thickness and (b) effective particle radius from ASTEX on June 17, 1992. The retrievals were limited to cases when $2 \leq \tau_c \leq 5$ and $4 \leq r_e \leq 26$ $\mu$m. This includes a total of $2.29 \times 10^4$ retrievals.

tion (PDF) (in percent) of retrieved cloud optical thickness and effective particle radius for various retrievals obtained using the MAS measurements shown in Figure 7. This includes a total of $2.29 \times 10^4$ retrievals in the range $2 \leq \tau_c \leq 5$ and $4 \leq r_e \leq 26$ $\mu$m. Figure 8a shows that the shape of the PDF for the retrieved cloud optical thickness is very similar for all three retrievals. However, there is clear evidence indicating that the Rayleigh scattering effects lead to overestimates of the cloud optical thickness at 0.66 $\mu$m for the optically thin pathes of the cloud scene. Results from both 0.66 $\mu$m (with correction) and 0.88 $\mu$m retrievals (without correction) are really identical, while the retrievals at 0.66 $\mu$m obtained without Rayleigh correction are shifted toward large values of $\tau_c$. The PDF of $\tau_c$ was shifted about 0.3 at $\tau_c = 3$ ($\Delta\tau_c = 10\%$) and 0.4 at $\tau_c = 4.4$ ($\Delta\tau_c = 9\%$), which is consistent with the results from our simulations. Figure 8b shows that for thin clouds, without making a Rayleigh correction at visible wavelength (0.66 $\mu$m), the retrieved cloud effective particle radius is also overestimated due to the overestimation of the cloud optical thickness. This phenomenon is easy to understand. For thin clouds the cloud effective particle radius increases as the cloud optical thickness increases for a given measured reflected radiance at the absorbing NIR 2.1 $\mu$m band. Increasing the cloud optical thickness enhances the reflected radiance contribution. Therefore the cloud needs to absorb more through increasing the water droplet size to keep the measured radiance at 2.1 $\mu$m unchanged. For thick clouds, however, the reflected radiance reaches its maximum in the asymptotic range for a given cloud effective particle radius, that is, photons can only "see" the cloud layer up to a maximum optical thickness value. Therefore, any more increase of $\tau_c$ does not change the reflected radiance at the TOC. It should be pointed out that the cloud optical thickness retrievals using a NIR wavelength (0.88 $\mu$m) are not completely error free, though they are much reduced over retrievals at 0.66 $\mu$m due to the much smaller Rayleigh scattering contributions at 0.88 $\mu$m. The errors in retrieved $\tau_c$ at 0.88 $\mu$m ranges from about 1 to 5% for $\tau_c$ between 2 and 5. We can see some differences in the PDF in retrieved $\tau_c$ between using band 0.66 $\mu$m (with Rayleigh correction) and 0.88 $\mu$m (without Rayleigh correction).

## 8. Discussion

As presented in section 7, Rayleigh scattering effects can be observed with satellite and/or airborne multichannel measurements. This can also be observed and validated with satellite multiangle measurements, e.g., the Multiangle Imaging Spectroradiometer (MISR) [*Diner et al.*, 1989] scheduled to be flown on the same platform as MODIS in 1998 [*King et al.*, 1995]. MISR consists of a set of nine cameras that view the Earth at nine angles (0, ±26.1°, ±45.6°, ±60.0°, and ±70.5° to the Earth's surface normal, where positive and negative angles refer to directions ahead of and behind the spacecraft, respectively) and in four spectral bands (0.443, 0.555, 0.670, and 0.865 $\mu$m). Thus, for a particular MISR band (e.g., 0.670 $\mu$m) we expect to observe Rayleigh scattering effects by looking at clouds with different viewing angles, that is, the smallest Rayleigh scattering effects are expected for nadir viewing ($\theta = 0°$) and the largest effects are expected for large viewing angles ($\theta = 70.5°$).

Our objective in this work is to accurately remove the Rayleigh scattering effects in cloud optical thickness retrievals. These unwanted Rayleigh scattering contributions, however, can be related to the cloud top pressure. It is particularly useful to relate Rayleigh scattering to cloud top pressure in remote sensing of cloud height and could potentially be utilized for this purpose by estimating the amount of Rayleigh scattering contributions above the cloud from visible radiance measurements. Obviously, for this purpose, one would like to use measured radiances at a short visible wavelength, e.g., the blue band, since the Rayleigh scattering contributions at this wavelength are more significant. Therefore it provides a sensitivity that could be applied to the remote retrieval of cloud top height using the measured radiance at the blue band. This will, however, be the topic of a future paper.

Since Rayleigh corrections have heretofore not been incorporated into satellite retrievals of cloud optical thickness, reported results are expected to be highly biased, especially at high latitudes. This effect will be incorporated into the cloud optical thickness and effective radius retrieval using MODIS data in 1998, where retrievals will be made using 0.65 $\mu$m over land, 0.86 $\mu$m over oceans, and 1.24 $\mu$m over snow and ice surface.

## 9. Conclusions

From studies of Rayleigh scattering effects on cloud optical thickness retrievals, we conclude that it is important to correct for Rayleigh scattering effects when retrieving cloud optical thickness for optically thin clouds and for thick clouds with large solar zenith angles ($\theta_0 \gtrsim 60°$). For thin clouds, however, errors in cloud optical thickness lead to errors in remotely retrieved cloud effective particle radius as well. By using a nonabsorbing NIR band (0.88 $\mu$m) in cloud optical thickness retrievals over oceans, the Rayleigh effects are much reduced because of the much smaller Rayleigh optical thickness. However, for cases with large solar zenith angles ($\theta_0 \gtrsim 60°$), $\Delta\tau_c$ in retrieved cloud optical thickness at $\lambda = 0.88$ $\mu$m still range between 5 and 25%. On the basis of single scattering theory, we have developed an iterative method to effectively remove the Rayleigh scattering contributions in cloud optical thickness retrievals. The iteration scheme is efficient and can be easily incorporated into any cloud retrieval algorithm. The correction scheme has been extensively tested with simulations for realistic cloud microphysical and optical properties and for a wide range of solar and viewing geometries. We conclude that the proposed Rayleigh correction algorithm can reduce the error in the retrieved cloud optical thickness in most cases from 20% to 2% for thin clouds. The error in retrieved $\tau_c$ was improved from a maximum of 28% in some cases to better than 4%. On the other hand, for optically thick clouds ($\tau_c \gtrsim 10$) and large solar zenith angles ($\theta_0 \approx 70°$) the error in $\tau_c$ was reduced in most cases from 12% to 2%. The improvements are even more substantial for cases of large $\tau_c$ and $\theta_0 = 80°$. Finally, we have validated the correction algorithm for thin clouds with experimental data obtained from the MODIS airborne simulator during ASTEX in June 1992.

## Appendix: Sensitivity Study of Equation (11)

### A1. Sensitivity of $C_m$ Value

The $C_m$ value in equation (11) was derived empirically from the simulations. Figures 9a and 9b give sample examples of $\Delta R_c$ for various $C_m$ values in (11) for cases of thin and thick clouds for different solar and viewing geometries. These are applicable to $\lambda = 0.66$ $\mu$m and $p_c/p_0 = 1$. $C_m = 1$ applies to

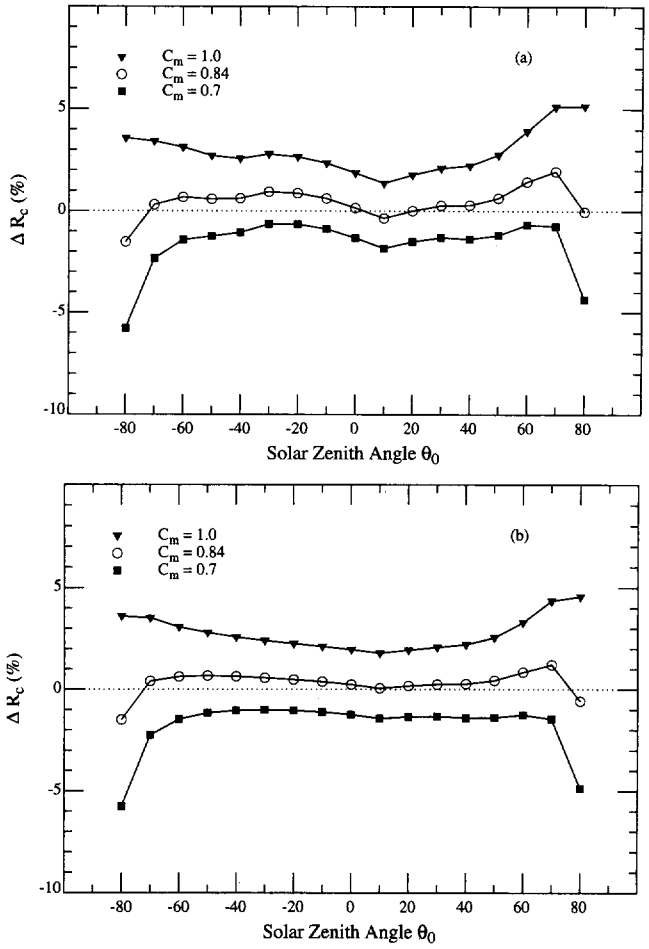


**Figure 9.** Error $\Delta R_c$ (in percent) for various $C_m$ values in (11) for $\theta = 45.2°$ and $\Delta\phi$ of 0° ($\theta_0 < 0°$) and 180° ($\theta_0 \geq 0°$) as a function of the solar zenith angle for (a) $\tau_c = 2$ and (b) $\tau_c = 10$.

the single scattering case (equation (9)) in which Rayleigh scattering was underestimated, whereas $C_m = 0.7$ overestimates the multiple scattering contributions. However, even for the single scattering approximation, (11) improves the accuracy of cloud optical thickness retrievals for cases of thin clouds and large solar zenith angles and all clouds. The most striking feature revealed in Figures 9a and 9b is that in the single scattering case the errors in cloud top reflectance are quite constant with various cloud optical thicknesses and different solar and viewing geometries. This led us to conclude that it is possible to modify $C_m$ value to best fit (11). Figures 9a and 9b show that except at very large solar zenith angle ($\theta_0 = 80°$), the $C_m$ value is a weak function of the solar and viewing geometry. Also, it only depends weakly on cloud optical properties as shown in Figures 9a and 9b, where the curves are very similar. In the following section A2, we will show that the $C_m$ value in (11) is nearly independent of the cloud top pressure $p_c$.

### A2. Clouds at High Altitude

To test the validity of (11) for different cloud top height, we take an extreme case where the cloud layer was located at $p_c/p_0 = 0.34$, that is, the cloud top pressure was about 345 hPa. Figures 10a and 10b present examples of $\Delta\tau_c$ for cases of both thin and thick clouds for different solar and viewing geometries. The $C_m = 0.84$ was used in all computations. Figures 10a and 10b are similar to Figures 5c and 5d except that now $p_c/p_0 = 0.34$ instead of 1. Again, Figures 10a and 10b show that (11) is very accurate but an estimate of $p_c/p_0$ is necessary for best results. The errors $\Delta\tau_c$ were corrected to within 1% in most cases. For the large solar zenith angles the Rayleigh scattering corrections are much more significant. Note that $p_c/p_0 = 0.34$ corresponds to $\tau_r = 0.015$ at $\lambda = 0.66$ $\mu$m. It is also equivalent to the Rayleigh optical thickness for $p_c/p_0 = 1.0$ at $\lambda = 0.88$ $\mu$m. Therefore, even for nonabsorbing NIR bands (0.88 $\mu$m), it is particularly important to correct for Rayleigh scattering effects in retrieved cloud optical thickness for large solar zenith angles ($\theta_0 \gtrsim 60°$).

### A3. Influences of Error in the Cloud Top Pressure

As discussed in section A2, our Rayleigh scattering correction scheme (equation (11)) is very accurate for any given cloud height level as long as one has cloud top pressure information. In reality, however, one can seldom get cloud top pressure to better than 100 hPa. We tested the sensitivity of (11) for different values of the cloud top pressure. Figures 11a–11d provide examples of these Rayleigh correction results resulting from errors in the cloud top height for cases of both thin and thick and low and high level cloud layers for different

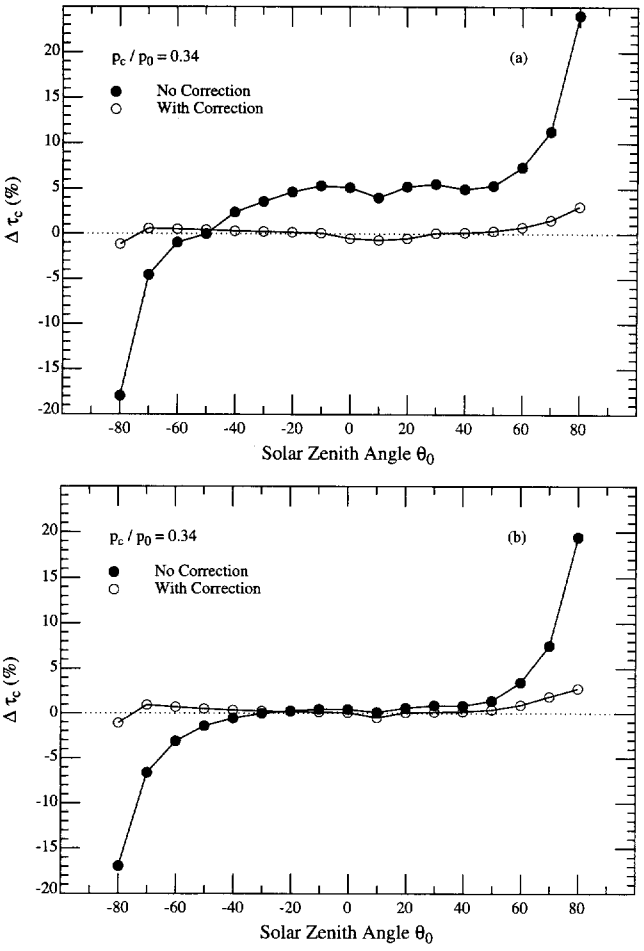


**Figure 10.** Error $\Delta\tau_c$ (in percent) for case of $p_c/p_0 = 0.34$ and $\theta = 45.2°$ and $\Delta\phi$ of 0° ($\theta_0 < 0°$) and 180° ($\theta_0 \geq 0°$) as a function of the solar zenith angle for (a) $\tau_c = 2$ and (b) $\tau_c = 10$.

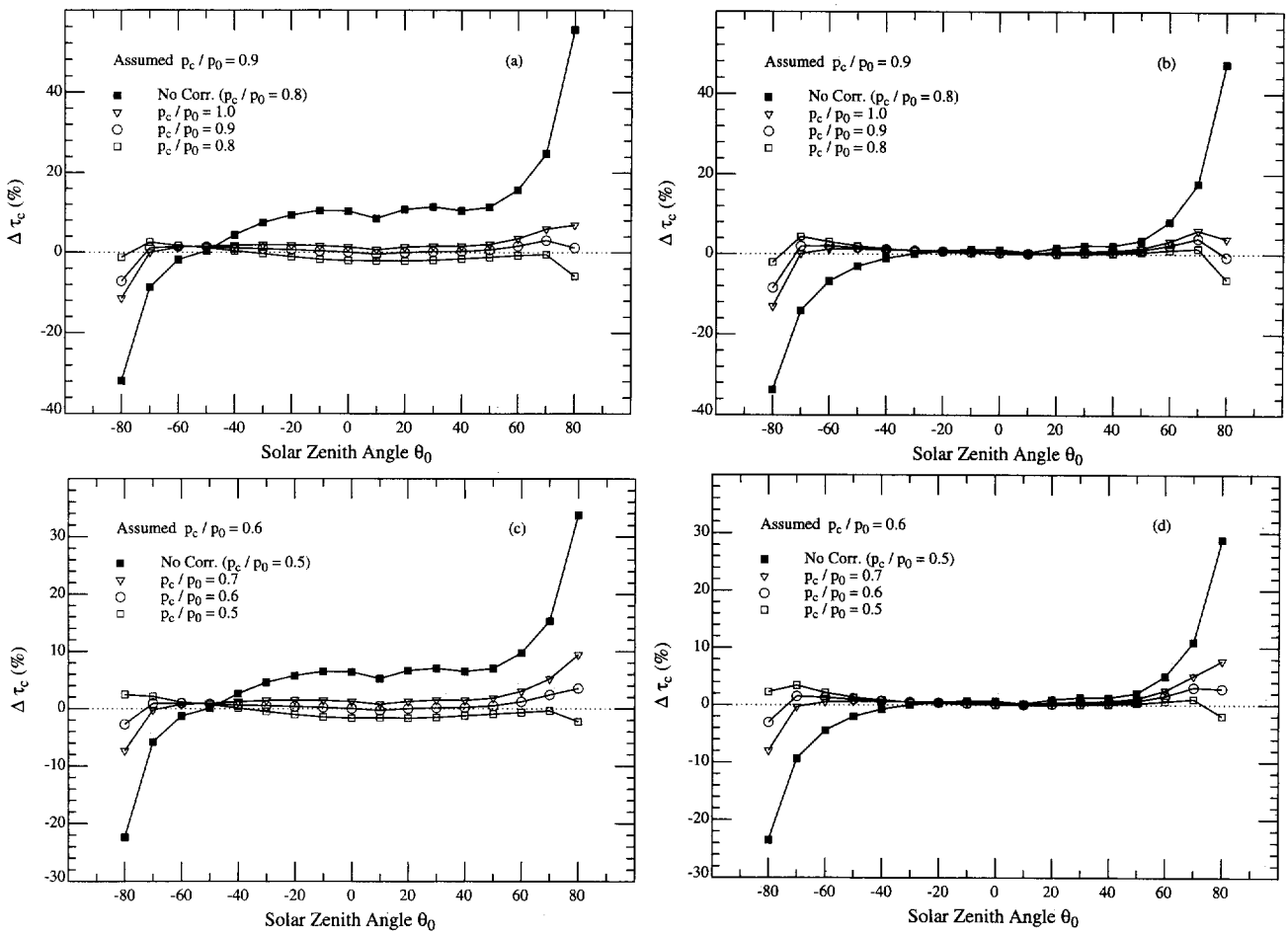


**Figure 11.** Error $\Delta\tau_c$ (in percent) with Rayleigh correction for various values of $p_c/p_0$ for $\theta = 45.2°$ and $\Delta\phi$ of 0° ($\theta_0 < 0°$) and 180° ($\theta_0 \geq 0°$) as a function of the solar zenith angle for (a) $\tau_c = 2$ (assumed $p_c/p_0 = 0.9$); (b) $\tau_c = 10$ (assumed $p_c/p_0 = 0.9$); (c) $\tau_c = 2$ (assumed $p_c/p_0 = 0.6$); and (d) $\tau_c = 10$ (assumed $p_c/p_0 = 0.6$). The Rayleigh correction was performed with assumed $p_c/p_0$ values.

solar and viewing geometries. In applying the Rayleigh correction, we assumed that the cloud layer was located at $p_c/p_0 = 0.9$ for Figures 11a and 11b and 0.6 for Figures 11c and 11d. The true $p_c/p_0$ values actually were 1.0, 0.9, and 0.8 in Figures 11a and 11b and 0.7, 0.6, and 0.5 in Figures 11c and 11d, respectively. Therefore the cloud top height was underestimated (overestimated) in the first (third) case. Note that an error of $\pm 0.1$ in $p_c/p_0$ corresponds to an error of $\pm 101$ hPa in the cloud top pressure. For comparison purposes, errors are also presented for cases without Rayleigh corrections for the smallest $p_c/p_0$ value in the figure. The errors in the other two cases (without corrections) are larger because of enhanced Rayleigh scattering contributions. Figure 11 shows that the Rayleigh correction scheme (11) is relatively insensitive to the errors in the cloud top pressure within $\pm 101$ hPa for both low and high level clouds. The results from correction in three different $p_c/p_0$ cases have almost no difference though the case for the correct $p_c/p_0$ value has over all a little better results.

**Acknowledgments.** One of the authors (M.W.) would like to thank H. R. Gordon of the University of Miami for his encouragement. We thank two anonymous reviewers for helpful comments. This research was supported by funding provided by the MODIS Science Team.

## References

Diner, D. J., et al., MISR: A multi-angle imaging spectroradiometer for geophysical and climatological research from EOS, *IEEE Trans. Geosci. Remote Sens.*, *27*, 200–214, 1989.

Foot, J. S., Some observations of the optical properties of clouds, I, Stratocumulus, *Q. J. R. Meteorol. Soc.*, *114*, 129–144, 1988.

Gordon, H. R., and M. Wang, Surface roughness considerations for atmospheric correction of ocean color sensors, 1, The Rayleigh scattering component, *Appl. Opt.*, *31*, 4247–4260, 1992.

Hansen, J. E., and L. D. Travis, Light scattering in planetary atmospheres, *Space Sci. Rev.*, *16*, 527–610, 1974.

King, M. D., Determination of the scaled optical thickness of clouds from reflected solar radiation measurements, *J. Atmos. Sci.*, *44*, 1734–1751, 1987.

King, M. D., D. D. Herring, and D. J. Diner, The Earth Observing System (EOS): A space-based program for assessing mankind's impact on the global environment, *Opt. Photonics News*, *6*, 34–39, 1995.

King, M. D., et al., Airborne scanning spectrometer for remote sensing of cloud, aerosol, water vapor and surface properties, *J. Atmos. Oceanic Technol.*, *13*, 777–794, 1996.

Nakajima, T., and M. D. King, Determination of the optical thickness and effective particle radius of clouds from reflected solar radiation measurements, I, Theory, *J. Atmos. Sci.*, *47*, 1878–1893, 1990.

Nakajima, T., and M. Tanaka, Matrix formulations for the transfer of solar radiation in a plane-parallel scattering atmosphere, *J. Quant. Spectrosc. Radiat. Transfer*, *35*, 13–21, 1986.

Nakajima, T. Y., and T. Nakajima, Wide-area determination of cloud

microphysical from NOAA AVHRR measurements for FIRE and ASTEX regions, *J. Atmos. Sci.*, *52*, 4043–4059, 1995.

Platnick, S., and F. P. J. Valero, A validation study of a satellite cloud retrieval during ASTEX, *J. Atmos. Sci.*, *52*, 2985–3001, 1994.

Twomey, S., and T. Cocks, Spectral reflectance of clouds in the near-infrared: Comparison of measurements and calculations, *J. Meteorol. Soc. Jpn.*, *60*, 583–592, 1982.

Twomey, S., and T. Cocks, Remote sensing of cloud parameters from spectral reflectance measurements in the near-infrared, *Beitr. Phys. Atmos.*, *62*, 172–179, 1989.

van de Hulst, H. C., *Multiple Light Scattering*, 739 pp., Academic, San Diego, Calif., 1980.

Wang, M., Atmospheric correction of the second generation ocean color sensors, Ph.D. dissertation, 135 pp., Univ. of Miami, Coral Gables, Fla., 1991.

M. D. King, Earth Sciences Directorate, NASA Goddard Space Flight Center, Greenbelt, MD 20771. (e-mail: king@climate.gsfc.nasa.gov)

M. Wang, University of Maryland Baltimore County, Code 970.2, NASA Goddard Space Flight Center, Greenbelt, MD 20771. (e-mail: wang@climate.gsfc.nasa.gov)

(Received December 19, 1996; revised July 31, 1997;
accepted August 4, 1997.)